ISME

Thermodynamic Assessment and Parametric Study of a Supercritical Thermal Power Plant

F. Ahmadi Boyaghchi*
Assistant Professor

A thermodynamic analysis of an operational 315 MW supercritical steam power plant (SPP) using the actual data is performed to assess the plant performance and identify the sites of energy losses and exergy destructions in each component of the plant. Various performance parameters such as component energy and exergy efficiencies, energy loss rate, exergy destruction rate, improvement potential (IP) rate and different plant efficiencies based on first and second thermodynamic laws were calculated and compared. Also, a parametric study is performed to investigate the effects of various turbine system operating conditions such as high pressure turbine (HPT) inlet pressure, HPT inlet temperature, intermediate pressure turbine (IPT) inlet pressure, HPT inlet temperature, and IPT inlet mass flow rate on plant efficiencies and exergy destruction of plant components.

Keywords: energy, exergy, sensitive study; steam power plant

1 Introduction

The steam power plants play a significant role for electricity generation using particularly natural gas as fossil fuel in Iran. Despite the growth of alternative energy technologies such as solar and wind power, it is expected that the natural gas and oil fuel will likely to remain substantial for decades in future. In fact, study on each thermal power plant for identifying the locations of losses in order to improvement is the major energy strategy in this country [1].
In this regard, exergy analysis method based on second law of thermodynamic is performed as an effective available energy auditing tool, which is recommended by other researchers [2-6]. This tool provides a better understanding of the process, sources of inefficiency, and quality of used energy as well as energy analysis. Zubair and Habib [7] carried out the second law thermodynamic analysis of the regenerative-reheat Rankine cycle power plants. Dincer and Muslim [8] performed the thermodynamic analysis of reheat cycle power plants using the energy and exergy analysis. Verkhivker and Kosoy [9] presented the system design and exergy analysis of power plants. Rosen [10] studied on energy and exergy analysis of coal-fired and nuclear thermal power plants. Suresh et al. [11] calculated the exergetic performance of the coal-based thermal power plants under subcritical, supercritical, and ultra-supercritical steam conditions. Datta et al. [12] analyzed exergy analysis of a coal fired steam power plant via three zones. Reddy and Butcher [13] investigated the second law of thermodynamics for

* Assistant Professor, Faculty of Engineering, Alzahra University, fahmadi@alzahra.ac.ir

waste heat recovery power generation system. Hasan et al. [14] analyzed thermodynamic inefficiencies for the considered coal-fired thermal power plants in Turkey and compared each plant to others. Ganapathy et al. [15] presented the energy and exergy losses of the individual apparatuses of the lignite fired thermal power plant. Aljundi [16] studied the performance of a steam power plant in Jordan and the energy and exergy losses for components in cycle. Oktay [17] presented exergy loss and proposed improving methods for a coal-fired thermal power plant in Turkey. Naterer et al. [18] analyzed the coal-fired thermal power plant with measured boiler and turbine losses. Kaushik and et al. [19] provides a review for coal-fired power plant and gas-fired combined cycle power plants. This review continues the previous studies. Hajidavalloo and Vosough [20] analyzed the energy and exergy methods for a supercritical power plant under different dead-state temperatures.
This work aims to identify and assess methods in order to determine the value of energy loss rate for increasing efficiencies of steam power plants, calculate different thermal and exergy efficiencies of the plant, and perform a parametric study to assess the effects of turbine system operating conditions on plant performance.

2 Materials and Methods

Figure (1) shows the one unit flow diagram of the conventional steam power plant (SPP) containing 6 units in Ahvaz, and table 1 indicates the properties of state numbers. The design basis of each unit is a nominal 315 MW supercritical water/steam cycle with a single reheating stage. The main plant consists of the following component groups: (1) steam generator or fossil boiler (FB) including an evaporator together with radiative superheater, a reheater, an economizer, and an air preheater which is supplied by natural gas (NG) (2) steam turbine system (TUR), (3) low pressure feed water heaters (LPH1, LPH2, LPH3, LPH4), and high pressure feed water heaters (HPH1, HPH2, HPH3) (4) two condensers (COD), and (5) three feedwater pumps (FWP). The steam turbine system consists of a high-pressure (HPT), an intermediate-pressure (IPT), and a low-pressure section (LPT). The high-pressure section is supplied with 23.5 MPa / 540^{o}C steam from the FB. The exhaust steam from the high-pressure turbine at 4.3 MPa is reheated to 540^{o}C in the steam generator and returns to the intermediate-pressure turbine (IPT). The IPT exhaust steam is then routed to the low-pressure steam turbine and from which it is condensed at the pressure of 6.5 MPa. Excluding the extraction steam from the high, intermediate, and low pressure section is used in low and high pressure feed water pre heaters (LPH1 to LPH4 and HPH1, HPH2, HPH3) for warming the feed water. The total three steam turbines generate 315 MW of power. The saturated mixture exhausted from the turbine condensates using the water-cooled condenser (COD) which operates at the pressure of 7.48 kPa. The cooling water flows into CON with the volumetric flow rate of 3600 m^3/hr and temperature of 25^{o}C, and exit at temperature of about 30^{o}C. The outflow from the condenser is pumped using two operating condensate pumps (CP) through the low-pressure feed water preheaters section (LPH1 to LPH4). The deaerator (DA) operates at 686.5 KPa. The booster pump (BP) delivered the feed water with pressure of 2.32 MPa to feed water pump (FWP). Finally, it supplies the feedwater to the high-pressure feedwater heaters (HPH1, HPH2, HPH3) of the steam generator at pressure of 32.85 MPa. The parasitic power such as BP, circulating pump in heater, condenser, air circulating fans, and other auxiliary consumption share in total 15% of net power generation in each unit according to plant data. Therefore, the net power output equating about 267.75 MW.

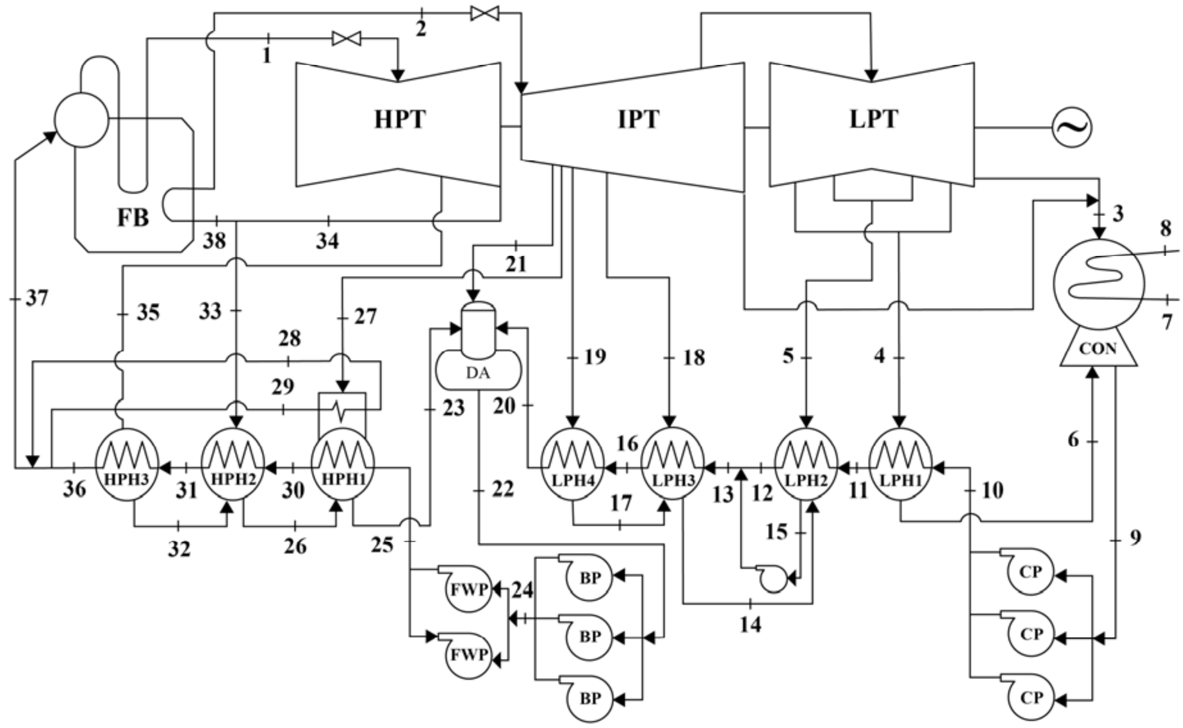

Figure 1 Flow diagram of the steam power plant (SPP)

The operation of the steam power plant is considered in the steady-state condition. The pressure loss throughout the pipelines is assumed negligible. NG such as methaneis used as the fuel with a lower heating value of 50,050 kJ/kg [2]. The fuel specific exergy is determined as: $x_{fuel}=\varphi\ LHV$, where φ is the exergy factor with value of 1.03 [2]. According to plant data, the combustion temperature is about 1350 K and the electricity consumption by FWPs and CPs is about 18 and 1.473 MW, respectively.

3 Analysis of Plant Components

For a steady state operation, the mass balance for each component is given by:

$$\sum_{i=1}^{n} \dot{m}_{in} = \sum_{i=1}^{n} \dot{m}_{out} \tag{1}$$

Where $\dot{m}$ is the mass flow rate. The energy rate is given by:

$$\dot{E} = \dot{m}_i \cdot (h_i - h_0) \tag{2}$$

Where h is specific enthalpy. The subscript i and 0 indicates the successive number of elements and dead-state condition, respectively.

Table 1 Thermodynamic properties, energy and exergy flow rates of state points in Figure 1

State point	Pressure P (kPa)	Temperature T (^oC)	Mass flow rate $\dot{m}$ (kJ/s)	Specific enthalpy h (kJ/kg)	Specific entropy s (kJ/ kg K)	Energy rate $\dot{E}$ (kW)	Exergy rate $\dot{E}x$ (kW)	Phase
1	23536.80	540.0	281.06	3322	6.183	904172	417068	Sup.
2	3921.81	540.0	230.97	3538	7.215	792861	321519	Sup.
3	6.57	35	131.31	146.6	0.505	5475	92.78	Sat. mix.
4	23.14	62	6.80	259.5	0.8562	1052	60.92	Sat. mix.
5	88.26	117.0	11.36	2712	7.511	29611	5428	Sup.
6	20.59	61.5	6.80	2612	7.901	17045	1779	Sub.
7	101.3	25	1000	104.89	0.3674	0	0	Sub.
8	101.3	30	1000	125.79	0.4369	20869	278.5	Sub.
9	24.51	37.86	183.75	158.50	0.5437	9863	215.3	Sub.
10	990.61	39.3	183.75	164.95	0.5711	11128	441.9	Sup.
11	982.43	58.5	183.75	246.6	0.8118	25872	1538	Sub.
12	900.12	96.3	183.75	404.1	1.2647	54976	5865	Sub.
13	873.23	93.3	215.16	393.97	1.2304	62198.45	6835.63	Sub.
14	224.58	103.7	20.05	434.58	1.3484	6610.28	745.86	Sub.
15	143.21	110	31.41	461.3	1.4185	1203.31	1351.4	Sat. Liq.
16	784.21	121.0	215.16	509.11	1.5383	86971.97	11857.46	Sub.
17	490.35	151.1	10.92	636.81	1.8448	5808.56	998.41	Sub.
18	230.46	234.0	9.13	2937.41	7.6057	25860.81	6157.36	Sup.
19	521.73	266.4	10.92	2993.56	7.3141	31544.27	8927.20	Sup.
20	707.08	148.9	215.16	628.02	1.8305	112556.65	18697	Comp.
21	1078.77	335.0	3.94	3118.28	7.000	12286.02	4081.36	Sup.
22	686.49	164.1	281.06	693.3	2.0419	165378.51	25056.49	Sup.
23	1569.12	179.9	61.52	762.8	2.1396	40474.62	7968.07	Sub.
24	2329.90	164.1	281.06	693.3	2.0419	165378.51	25056.49	Sub.
25	32853.45	169.9	281.06	738.1	2.0419	177970.00	37647.98	Sub.
26	4134.63	207.5	49.50	887.18	2.4014	38895.45	8743.26	Sub.
27	1647.57	414.1	11.80	3283.2	7.2661	37504.05	13233.22	Sup.
28	26003.32	289.5	55.55	1276.13	3.1547	65062.38	18898.11	Sup.
29	26312.43	279.5	55.55	1227.15	3.0581	62341.54	17777.49	Sub.
30	30523.45	197.5	281.06	855.78	2.3072	211045.14	48491.28	Sub.
31	28223.45	250.5	281.06	1091.08	2.7972	260314.96	73564.64	Sub.
32	6512.82	260.5	20.06	1136.71	2.8382	20698.30	13862.24	Sub.
33	4134.63	299.4	29.63	2955.46	6.6112	84547.90	29333.14	Sup.
34	4324.80	301.7	260.62	2955.46	6.3111	742915.55	281065.63	Sup.
35	6784.48	358.6	20.06	3050.08	6.2887	59080.51	23665.78	Sup.
36	26312.43	279.5	281.06	1227.15	3.06193	315422.39	89624.41	Sub.
37	26312.43	281.5	280.69	1236.78	3.0806	317710.20	90646.02	Sub.
38	4256.23	301.7	83.80	2955.27	6.3001	238877.76	90633.51	Sup.
0	101.3	298.15	-	104.89	0.3674	0	0	Ref.

Sub.: subcooled liquid, Sup.: superheat, Sat. mix.: saturated mixture, Ref.:reference (or dead-state)

Depending on the applications of a system, energy efficiency can be defined in several ways. In this study energy efficiency and energy loss are calculated using the following definitions [21]:

$$\eta = \frac{\dot{E}_{recoverd}}{\dot{E}_{expended}} \tag{3}$$

$$\dot{L} = \dot{E}_{expened} - \dot{E}_{recoverd} \tag{4}$$

Where η is the energy efficiency and $\dot{L}$ is the energy loss rate (Table 2).
The exergy rate is expressed by

$$\dot{E}x = \dot{m}_i \cdot [(h_i - h_0) - T_0(s_i - s_0)] \tag{5}$$

Where $\dot{E}x$, T, h and s indicate the total exergy rate, temperature, enthalpy and entropy, respectively. The subscript 0 shows the dead-state condition.
Similarly, the exergy efficiency for a system can be calculated in different approaches. The exergy efficiency and exergy destruction are obtained by [21]

$$\varepsilon = \frac{\dot{E}x_{recoverd}}{\dot{E}x_{expended}} \tag{6}$$

$$\dot{I} = \dot{E}x_{expened} - \dot{E}x_{recoverd} \tag{7}$$

Where ε and $\dot{I}$ are exergy efficiency and exergy destruction rate, respectively (Table 2).
Energy efficiency of the plant is estimated by the below formula [21]:

$$\eta_{plant-1} = \frac{\dot{E}_{net,out}}{\dot{E}_{in}} \tag{8}$$

Where $\dot{E}_{net,out}$ and $\dot{E}_{in}$ are the net output and the input energy rates, respectively and can be indicated by:

$$\dot{E}_{net,out} = \dot{W}_{TUR} - \dot{W}_{parasitic\ power} \tag{9}$$

$$\dot{E}_{in} = (\dot{E}_1 - \dot{E}_{37}) + (\dot{E}_2 - \dot{E}_{38}) \tag{10}$$

Where $\dot{W}_{TUR}$ indicates the electricity generation and $\dot{W}_{parasiticpower}$ refers to the auxiliary devices consuming 15% of net power generation. $\dot{E}$ denotes the energy rate and subscripts indicate state points in Figure 1.

Table 2 Expressions of energy efficiency and energy loss rate for each component

Item	Energy loss rate	Energy efficiency
FB	$\dot{L}_{FB} = \dot{m}_{fuel}LHV + (\dot{E}_{37} + \dot{E}_{38}) - (\dot{E}_1 + \dot{E}_2)$	$\eta_{FB} = \frac{(\dot{E}_1 - \dot{E}_{37}) + (\dot{E}_2 - \dot{E}_{38})}{\dot{m}_{fuel}LHV}$
TUR	$\dot{L}_{TUR} = (\dot{E}_1 + \dot{E}_2) - (\dot{E}_{extr.} + \dot{E}_3 + \dot{W}_{TUR})$ $\dot{E}_{extr.} = \dot{E}_{35} + \dot{E}_{34} + \dot{E}_{27} + \dot{E}_{21} + \dot{E}_{19} + \dot{E}_{18} + \dot{E}_5 + \dot{E}_4$	$\eta_{TUR.} = \frac{\dot{W}_{TUR}}{(\dot{E}_1 + \dot{E}_2) - (\dot{E}_{extr.} + \dot{E}_3)}$
CON	$\dot{L}_{CON} = (\dot{E}_3 + \dot{E}_6 + \dot{E}_7) - (\dot{E}_8 + \dot{E}_9)$	$\eta_{CON} = \frac{\dot{E}_8 - \dot{E}_7}{\dot{E}_3 + \dot{E}_6 - \dot{E}_9}$

CP	$\dot{L}_{CP} = \dot{W}_{CP} + \dot{E}_9 - \dot{E}_{10}$	$\eta_{CP} = \frac{\dot{E}_{10} - \dot{E}_9}{\dot{W}_{CP}}$
LPH1	$\dot{L}_{LPH1} = \left(\dot{E}_4 + \dot{E}_{10}\right) - \left(\dot{E}_6 + \dot{E}_{11}\right)$	$\eta_{LPH1} = \frac{\dot{E}_{11} - \dot{E}_{10}}{\dot{E}_4 - \dot{E}_6}$
LPH2	$\dot{L}_{LPH2} = \left(\dot{E}_5 + \dot{E}_{14} + \dot{E}_{11}\right) - \left(\dot{E}_{15} + \dot{E}_{12}\right)$	$\eta_{LPH2} = \frac{\dot{E}_{12} - \dot{E}_{11}}{\left(\dot{E}_5 + \dot{E}_{14}\right) - \dot{E}_{15}}$
LPH3	$\dot{L}_{LPH3} = \left(\dot{E}_{13} + \dot{E}_{17} + \dot{E}_{18}\right) - \left(\dot{E}_{14} + \dot{E}_{16}\right)$	$\eta_{LPH3} = \frac{\dot{E}_{16} - \dot{E}_{13}}{\left(\dot{E}_{17} + \dot{E}_{18}\right) - \dot{E}_{14}}$
LPH4	$\dot{L}_{LPH4} = \left(\dot{E}_{16} + \dot{E}_{19}\right) - \left(\dot{E}_{17} + \dot{E}_{20}\right)$	$\eta_{LPH4} = \frac{\dot{E}_{20} - \dot{E}_{16}}{\dot{E}_{19} - \dot{E}_{17}}$
DA	$\dot{L}_{DA} = \left(\dot{E}_{20} + \dot{E}_{21} + \dot{E}_{23}\right) - \dot{E}_{22} + \dot{m}_{23}e_{21} + \dot{m}_{21}e_{23}$	$\eta_{DA} = \frac{\dot{m}_{20}\left(e_{22} - e_{20}\right)}{\left(\dot{m}_{21} + \dot{m}_{23}\right)\left(e_{21} + e_{23} - e_{22}\right)}$
FWP	$\dot{L}_{FWP} = \dot{W}_{FWP} + \dot{E}_{24} - \dot{E}_{25}$	$\eta_{FWP} = \frac{\dot{E}_{25} - \dot{E}_{24}}{\dot{W}_{FWP}}$
HPH1	$\dot{L}_{HPH1} = \left(\dot{E}_{25} + \dot{E}_{26} + \dot{E}_{27} + \dot{E}_{29}\right) - \left(\dot{E}_{23} + \dot{E}_{28} + \dot{E}_{30}\right)$	$\eta_{HPH1} = \frac{\left(\dot{E}_{30} - \dot{E}_{25}\right) + \left(\dot{E}_{28} - \dot{E}_{29}\right)}{\left(\dot{E}_{27} + \dot{E}_{26}\right) - \dot{E}_{23}}$
HPH2	$\dot{L}_{HPH2} = \left(\dot{E}_{30} + \dot{E}_{32} + \dot{E}_{33}\right) - \left(\dot{E}_{31} + \dot{E}_{26}\right)$	$\eta_{HPH2} = \frac{\left(\dot{E}_{31} - \dot{E}_{30}\right)}{\left(\dot{E}_{32} + \dot{E}_{33}\right) - \dot{E}_{26}}$
HPH3	$\dot{L}_{HPH3} = \left(\dot{E}_{36} + \dot{E}_{32}\right) - \left(\dot{E}_{31} + \dot{E}_{35}\right)$	$\eta_{HPH3} = \frac{\dot{E}_{36} - \dot{E}_{31}}{\dot{E}_{35} - \dot{E}_{32}}$

This efficiency (Eq. (8)) does not include the losses of furnace-boiler system. For incorporating these losses, the energy efficiency of the plant can be expressed as [21]:

$$\eta_{plant-2} = \frac{\dot{W}_{net,out}}{\dot{m}_{fuel} LHV} \tag{11}$$

Where $\dot{m}_{fuel}$ and LHV indicate the mass flow rate and the lower heating value of fuel, respectively.

Table 3 Expressions of exergy efficiency and exergy destruction rate for each component

Item	Exergy destruction	Exergy efficiency
FB	$\dot{I}_{FB} = \dot{m}_{fuel}x + \left(\dot{E}x_{37} + \dot{E}x_{38}\right) - \left(\dot{E}x_1 + \dot{E}x_2\right)$	$\varepsilon_{FB} = \frac{(\dot{E}x_1 - \dot{E}x_{37}) + (\dot{E}x_2 - \dot{E}x_{38}}{\dot{m}_{fuel}x}$
TUR	$\dot{I}_{TUR} = \left(\dot{E}x_1 + \dot{E}x_2\right) - \left(\dot{E}x_{extr.} + \dot{E}x_3 + \dot{W}_{TUR}\right)$ $\dot{E}x_{extr.} = \dot{E}x_{35} + \dot{E}x_{34} + \dot{E}x_{27} + \dot{E}x_{21} + \dot{E}x_{19} + \dot{E}x_{18} + \dot{E}x_5 + \dot{E}x_4$	$\varepsilon_{TUR} = \frac{\dot{W}_{TUR}}{(\dot{E}x_1 + \dot{E}x_2) - (\dot{E}x_{extr.} + \dot{E}}$
CON	$\dot{I}_{CON} = \left(\dot{E}x_3 + \dot{E}x_6 + \dot{E}x_7\right) - \left(\dot{E}x_8 + \dot{E}x_9\right)$	$\varepsilon_{CON} = \frac{\dot{E}x_8 - \dot{E}x_7}{\dot{E}x_3 + \dot{E}x_6 - \dot{E}x_9}$
CP	$\dot{I}_{CP} = \dot{W}_{CP} + \dot{E}x_9 - \dot{E}x_{10}$	$\varepsilon_{CP} = \frac{\dot{E}x_{10} - \dot{E}x_9}{\dot{W}_{CP}}$

LPH1	$\dot{I}_{LPH\,1} = \left(\dot{E}x_4 + \dot{E}x_{10}\right) - \left(\dot{E}x_6 + \dot{E}x_{11}\right)$	$\varepsilon_{LPH1} = \dfrac{\dot{E}x_{11} - \dot{E}x_{10}}{\dot{E}x_4 - \dot{E}x_6}$
LPH2	$\dot{I}_{LPH\,2} = \left(\dot{E}x_5 + \dot{E}x_{14} + \dot{E}x_{11}\right) - \left(\dot{E}x_{15} + \dot{E}x_{12}\right)$	$\varepsilon_{LPH2} = \dfrac{\dot{E}x_{12} - \dot{E}x_{11}}{\left(\dot{E}x_5 + \dot{E}x_{14}\right) - \dot{E}x_{15}}$
LPH3	$\dot{I}_{LPH\,3} = \left(\dot{E}x_{13} + \dot{E}x_{17} + \dot{E}x_{18}\right) - \left(\dot{E}x_{14} + \dot{E}x_{16}\right)$	$\varepsilon_{LPH3} = \dfrac{\dot{E}x_{16} - \dot{E}x_{13}}{\left(\dot{E}x_{17} + \dot{E}x_{18}\right) - \dot{E}x_{14}}$
LPH4	$\dot{L}_{LPH\,4} = \left(\dot{E}_{16} + \dot{E}_{19}\right) - \left(\dot{E}_{17} + \dot{E}_{20}\right)$	$\eta_{LPH4} = \dfrac{\dot{E}_{20} - \dot{E}_{16}}{\dot{E}_{19} - \dot{E}_{17}}$
DA	$\dot{L}_{DA} = \left(\dot{E}x_{20} + \dot{E}x_{21} + \dot{E}x_{23}\right) - \dot{E}x_{22} + \dot{m}_{23}ex_{21} + \dot{m}_{21}ex_{23}$	$\varepsilon_{DA} = \dfrac{\dot{m}_{20}\left(ex_{22} - ex_{20}\right)}{\left(\dot{m}_{21} + \dot{m}_{23}\right)\left(ex_{21} + ex_{23} -\right.}$
FWP	$\dot{I}_{FWP} = \dot{W}_{FWP} + \dot{E}x_{24} - \dot{E}x_{25}$	$\varepsilon_{FWP} = \dfrac{\dot{E}x_{25} - \dot{E}x_{24}}{\dot{W}_{FWP}}$
HPH1	$\dot{I}_{HPH\,1} = \left(\dot{E}x_{25} + \dot{E}x_{26} + \dot{E}x_{27} + \dot{E}x_{29}\right) - \left(\dot{E}x_{23} + \dot{E}x_{28} + \dot{E}x_{30}\right)$	$\varepsilon_{HPH1} = \dfrac{\left(\dot{E}x_{30} - \dot{E}x_{25}\right) + \left(\dot{E}x_{28} -\right.}{\left(\dot{E}x_{27} + \dot{E}x_{26}\right) - \dot{E}x_2}$
HPH2	$\dot{I}_{HPH\,2} = \left(\dot{E}x_{30} + \dot{E}x_{32} + \dot{E}x_{33}\right) - \left(\dot{E}x_{31} + \dot{E}x_{26}\right)$	$\varepsilon_{HPH2} = \dfrac{\left(\dot{E}x_{31} - \dot{E}x_{30}\right)}{\left(\dot{E}x_{32} + \dot{E}x_{33}\right) - \dot{E}x_{26}}$
HPH3	$\dot{I}_{HPH\,3} = \left(\dot{E}x_{36} + \dot{E}x_{32}\right) - \left(\dot{E}x_{31} + \dot{E}x_{35}\right)$	$\varepsilon_{HPH3} = \dfrac{\dot{E}x_{36} - \dot{E}x_{31}}{\dot{E}x_{35} - \dot{E}x_{32}}$

Exergy efficiency of the plant can be obtained from several approaches such as $\varepsilon_{plant-1}$, $\varepsilon_{plant-2}$ and $\varepsilon_{plant-3}$ estimated by the following formula [21]:

$$\varepsilon_{plant-1} = \frac{\dot{E}x_{net,out}}{\dot{E}x_{in}} \tag{12}$$

Where ε, $\dot{E}x_{net,out}$ and $\dot{E}x_{in}$ are exergy efficient, the net output and the input exergy rates, respectively and can be expressed as follows:

$$\dot{E}x_{net,out} = \dot{W}_{TUR} - \dot{W}_{parasiticload} \tag{13}$$

$$\dot{E}x_{in} = \left(\dot{E}x_1 - \dot{E}x_{37}\right) + \left(\dot{E}x_2 - \dot{E}x_{38}\right) \tag{14}$$

In this approach, the irreversibility due to fuel combustion in furnace and exergy losses associated with hot exhaust gases was not included.

$$\varepsilon_{plant-2} = \frac{\dot{E}x_{net,out}}{\dot{E}_{in}\left(1 - \dfrac{T_0}{T_{FB}}\right)} \tag{15}$$

Where T_0 and T_{FB} are the dead-state or environment temperature and furnace temperature, respectively, and $\dot{E}_{in}$ can be obtained from Eq. (6).This definition includes the irreversibility of heat transfer from furnace to the steam. Also, the exergy efficiency of plant can be defined as

$$\varepsilon_{plant-3} = \frac{\dot{E}_{net,out}}{\dot{m}_{fuel} x_{fuel}} \tag{16}$$

Where x_{fuel} is the specific exergy of the fuel.

4 Energy and Exergy Analysis of Combustion Products

Exhaust gas is the mixture of various gases. Table 4 shows the molar analysis of combustion products obtained from technical data. According the power plant report the exhaust gas temperature and pressure are 425.15 K and 1.013 bar, respectively.

Table 4 Exhaust gas analysis (obtained from technical data)

Component	N_2	O_2	CO_2	H_2O
x (Vol %)	0.7579	0.1208	0.0407	0.0806

4-1 Energy Loss Analysis of Exhaust Gas

The amount of energy loss from stack can be calculated by following formulas [2,3]:

$$E_{mix} = \frac{\dot{m}}{M_{mix}} \overline{c}_{p,mix} \left(T_{mix} - T_0\right) \tag{17}$$

$$M_{mix} = \sum x_k M_k \tag{18}$$

$$\overline{c}_{p,mix} = \sum x_k \overline{c}_{p,k} \tag{19}$$

Where $\dot{m}$, $\overline{c}_p$, T, x and M are mass flow rate of fuel and air into FB, molar specific heat at pressure constant, temperature, molar fraction and molar mass respectively. The subscripts mix, 0 and k indicate gas mixture, dead state and each component of combustion products, respectively.

For $298.15K < T \leq T_{max}$, P_{ref}=1 bar with y=10^{-3}T, the specific heat for components in exhaust gas can be calculated by following relation [3]:

$$\overline{c}_p = a + by + cy^{-2} + dy^2 \tag{20}$$

Where a, b, c, and d can be obtained for various components from Table (5).

Table 5 The values of coefficients in Eq. (20)

Components	a	b	c	d
N_2	30.418	2.544	-0.238	-
O_2	29.154	6.477	-0.184	1.017
CO_2	51.128	4.368	-1.469	-
H_2O	34.376	7.841	-0.423	-

The energy loss of exhaust gas is calculated according to Table (4) and (5) and Eqs (17) to (20).

4-2 Exergy Loss Analysis of Exhaust Gas

Exergy loss of exhaust gas consists of physical and chemical exergies. The molar physical exergy of gas mixture can be obtained from [2, 3]:

$$\dot{E}x_{mix}^{PH} = \frac{\dot{m}}{M_{mix}}\left[\left(\bar{h}_{mix} - \bar{h}_0\right) - \left(\bar{s}_{mix} - \bar{s}_0\right)\right] \tag{21}$$

$$\bar{h}_{mix} = \sum_{k=1}^{N} x_k \overline{h_k} = \sum_{k=1}^{N} x_k \left(\bar{h}_{f,k}^{\circ} + \Delta\bar{h}_k\right) \tag{22}$$

$$\bar{s}_{mix} = \sum_{k=1}^{N} x_k \overline{s_k} \tag{23}$$

$$\bar{s}_k\left(T, x_k, P_0\right) = \bar{s}_k^{\circ}\left(T\right) - \bar{R}\,Ln\left(\frac{x_k P_0}{P_{ref}}\right) \tag{24}$$

Where $\bar{h}_{mix}$ and $\bar{s}_{mix}$ are molar enthalpy and entropy of gas mixture at T and P, $\dot{m}$ is the mass flow rate of fuel and air and M_{mix} is molar mass of gas mixture. In Eqs. (22) to (24), x_k is the mole fraction of combustion products in exhaust gas which is obtained from Table 4. $\bar{h}_{f,k}^{\circ}$ is the enthalpy formation of each component in gas mixture. $\bar{s}_k^{\circ}$ is standard molar entropy of each component, and $\bar{R}$ universal gas constant. Table (6) summarizes data for enthalpy (in kJ/kmol) and entropy (in kJ/kmol. K) at state of exhaust gas. Values are obtained from Eqs. (22) to (24).

Table 6 The value of molar enthalpy and entropy of exhaust gas

Component	N_2	O_2	CO_2	H_2O	Mixture
$\bar{h}_f^{\circ}$ (kJ/kmol)	0	0	-393522	-241827	-
$\Delta\bar{h}$ (kJ/kmol)	3706.25	5308.25	7088.5	4319	-
$\bar{h}_{mix}$ (kJ/kmol)	-	-	-	-	-31450
$\bar{s}^{\circ}$ (kJ/kmol. K)	202.17	215.87	227.83	200.53	-
$\bar{s}$ (kJ/kmol. K)	204.4	233.3	253.8	221.4	-
$\bar{s}_{mix}$ (kJ/kmol. K)	-	-	-	-	211.2

Special considerations apply for the combustion products. When a mixture is brought to p_o, T_o, some condensation would occur: At 25°C, 1 atm, the mixture would consist of N_2, O_2, and CO_2, together with saturated water vapor in equilibrium with saturated liquid.
On the basis of 1 kmol of combustion products formed, the gas phase at 25°C would consist of 0.9193 kmol of dry products (0.7507 N_2, 0.1208 O_2, 0.0407 CO_2,) plus n_v kmol of water vapor. The partial pressure of water vapor would be equal to the saturation pressure, p_g (25°C) = 0.0317 bar. The amount of water vapor present can be found from [3]:

$$n_{\upsilon} = \frac{n_g P_g}{P_{ref} - P_g} \tag{25}$$

Where n_g is the amount of gas phase in combustion products which is equal 0.9194 kmol, P_g is saturation pressure at 25°C, and P_{ref} is reference pressure.
On the basis of 1 kmol of mixture, the composition at 25°C, 1 atm would be

$\underline{0.7507\ N_2,\ 0.1208\ O_2,\ 0.0407\ CO_2,\ 0.0297\ H_2O(g)}$, $0.0510\ H_20(l)$

The mole fractions of the components of the gas phase, shown underlined, are
x' N_2 = 0.7970, x' O_2 = 0.1282, x' CO_2 = 0.0433, x' $H_2O(g)$ = 0.0315
Enthalpy and entropy of dead state can be calculated by:

$$\bar{h}_0 = \sum x_k \bar{h}^o_{f,k} \tag{26}$$

$$\bar{s}_0 = \sum x_k \bar{s}'_{0,k}\left(T_0, x'_k, P_0\right) = \sum x_k \left[\bar{s}^\circ_k\left(T_0\right) - \bar{R}\, Ln\left(\frac{x'_k P_0}{P_{ref}}\right)\right] \tag{27}$$

Where x'_k mole fraction of components in gas phase.

Table 7 The values of enthalpy and entropy at dead state

Component	**N_2**	**O_2**	**CO_2**	**$H_2O(g)$**	**$H_2O(l)$**	**Mixture**
$\bar{h}_0$ **(kJ/kmol)**	-	-	-	-	-	-37776.7
$\bar{s}'_0$ **(kJ/kmol. K)**	203.9	232.8	253.8	229.2	69.94	-
$\bar{s}_0$ **(kJ/kmol. K)**	-	-	-	-	-	201.9

According to Table (6) and (7) and Eq. (20) the physical Exergy of exhaust gas is calculated 2818 kJ/kmol. The chemical exergy of exhaust gas can be divided to gaseous and liquid phases. The chemical exergy of gas mixture can be obtained by following equation:

$$\overline{ex}^{CH}_{mix} = \left(\sum x'_k \overline{ex}^{CH}_k + \bar{R} T_0 \sum x'_k Ln x'_k\right) \tag{28}$$

On the basis of 1 kmol of mixture, we have 0.949 kmol as a gas phase and 0.051 kmol as liquid water; thus $\overline{ex}$ = 0.949(187.7) + 0.051(45)=180.6 kJ/kmol. Finally, the chemical exergy rate of the combustion products equals 0.65 MW.

5 Results and Discussion

The thermodynamic properties of water including pressure, temperature, energy and exergy rates at state points (Figure 1) were calculated and listed in Table (1). The dead-state pressure and temperature (denoted 0) are considered 101.3 kPa and 298.15 K, respectively.

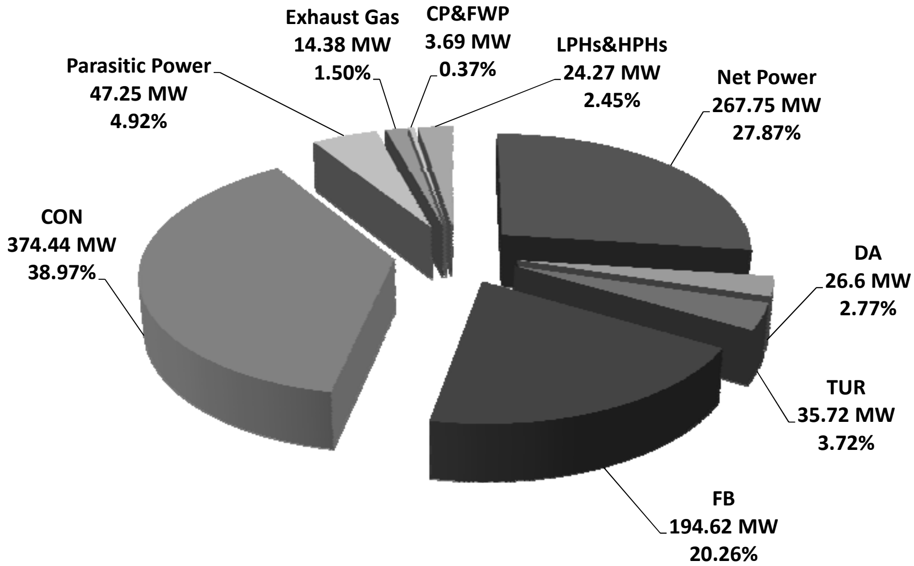

Figure 2 Energy loss diagram. Given as the percentages of plant energy input (988.32 MW)

An investigation of the energy pie diagram (Figure 2) shows that 38.4% of the energy of fuel is rejected in CON, 19.9% of it is lost in FB, and only 27.4% of it is converted to power.
As it is obvious from table (4), CON has the lowest thermal efficiency with the value of 36.7% among the observed components of the plant whereas the thermal efficiency of other devices has a good condition.
The first law efficiency of the plant is calculated to be 35.32% [Eq.(10)] base on the ratio of the energy input to the steam which is not considered the energy losses in FB and 27.4% [Eq.(11)] based on the ratio of the energy input to the plant. This results in wasting more than 72% of thermal energy of NG. An exergy pie diagram is illustrated (Figure 3) to identify the locations of exergy destruction and quantify those losses in the plant.
The values for energy loss rates and energy efficiency of the identified locations (Figure 2) are summarized in Table (4).

Table 4 Energetic performance data determined for one representative unit of plant

Item	Energy efficiency (%)	Energy loss rate or Power (MW)
CON	36.7	374.447
FB	75.2	194.627
TUR	78.5	35.427
DA	78.8	26.608
HPH2	81.1	17.080
LPH2	82.3	6.173
FWP	78.6	3.408
LPH1	98.02	0.302
CP	80.4	0.287
LPH3	98.8	0.285
LPH4	99.4	0.151
HPH3	99.6	0.146
HPH1	99.6	0.128
Parasitic power	-	47.25
Plant	$35.32^{\text{Eq. (10)}}$ $27.40^{\text{Eq. (11)}}$	267.75

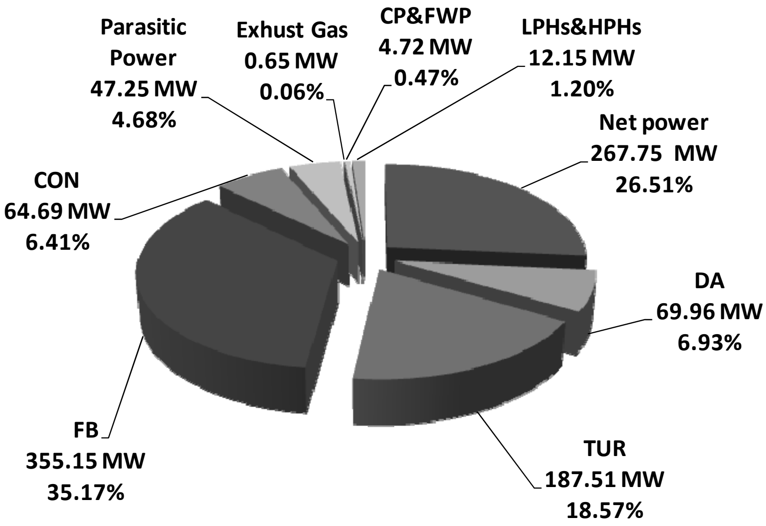

Figure 3 Exergy destruction diagram. The numbers are given as the percentages of the plant exergy input (1006.83 MW)

As this power plant uses the water cooled condenser to condense the exhaust steam of the turbine, the main improvement achieving in CON is lowering the coolant temperature.

Table 5 Exergetic performance data for one representative unit of plant

Item	Exergy efficiency (%)	Exergy destruction rate or power (MW)	Improvement potential rate (MW)
FB	35.5	355.15	275.551
TUR	63.4	187.51	227.13
DA	70.2	69.964	56.950
CON	34.5	64.690	11.062
HPH2	60.3	4.888	0.801
FWP	67.7	3.408	0.729
HPH1	70.4	2.044	0.298
HPH3	77.3	1.703	0.165
LPH3	78.3	1.388	0.301
CP	73.3	1.315	1.174
LPH4	82.2	1.089	0.152
LPH2	81.2	0.701	0.103
LPH1	85.3	0.339	0.066
Parasitic power	-	47.25	-
Plant	48.10 $^{\text{Eq. (12)}}$ 32.14 $^{\text{Eq. (15)}}$ 26.50 $^{\text{Eq. (16)}}$	267.75	-

From the Figure (3), It is observed that exergy destruction rate of FB is dominant over all other irreversibilities in plant. It exclusively represents 35.2% of losses in the cycle. This indicates that chemical reaction is a high source of irreversibility while the exergy destruction rate CP and FWP are only 0.5% of total exergy destruction. Moreover, investigation shows that 18.6% of exergy destruction occurs in TUR system. Exergy destructions and exergy efficiencies for one unit are calculated and summarized in Table (5). It is found that FB and LPH1 with the exergy efficiencies of 35.5% and 90.3% are the least and the most efficient devices in the plant. Energy and exergy studies indicate that the significant improvements shall be existed in FB, although the heat loss rate in CON is dominant. Optimization of FB can be achieved by selecting the better materials for furnace alongside improving the combustion process. The inefficiencies of combustion can be reduced by preheating the combustion air and reducing the air–fuel ratio.

The calculated exergy efficiencies of the plant is 48.10% [Eq.(12)] based on the energy input to the working fluid which is not included the irreversibilities in FB, 32.14% [Eq.(15)] based on heat transfer which is included the irreversibilities during energy transfer from furnace to the steam, and 26.5% [Eq.(16)] based on exergy input to the plant associated with combustion process and exergy lost with exhaust gases. In addition, improvement potential (IP) is calculated by the following formula [22]:

$$IP = (1-\varepsilon)\left(\dot{E}_{in} - \dot{E}_{out}\right) \tag{17}$$

Results indicate the high improvement potential for FB and TUR system.

As a part of analysis, a parametric study is performed based on Eq. (10) and Eq. (16) for investigating the effect of various operating conditions of TUR on energy and exergy efficiencies of the plant. Figure (4) and Figure (5) represent the constant steam mass flow rate and fuel input. Both energy and exergy efficiencies increase as the HPT inlet pressure and temperature rise. This is because of the greater energy/exergy content of a steam resulting in higher power output of the turbine.

As shown in Figure (6), there is no significant growth observed in the plant performance due to the high IPT inlet temperature. The reason for the slow incremental process is the low mass flow rate at IPT inlet compared to the flow rate at HPT inlet.

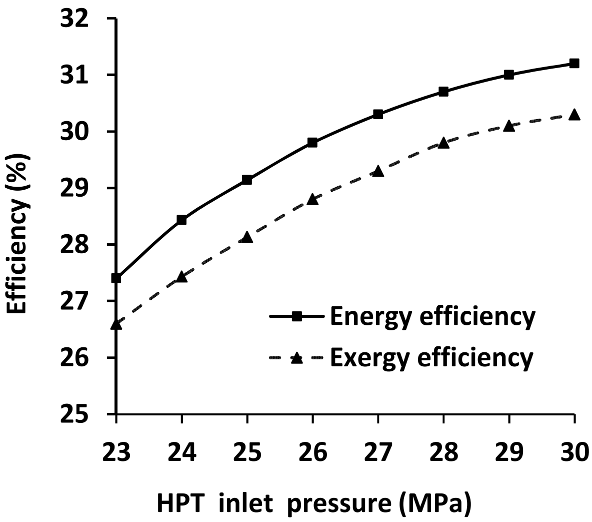

Figure 4 Variations of energy and exergy efficiencies versus HPT inlet pressure

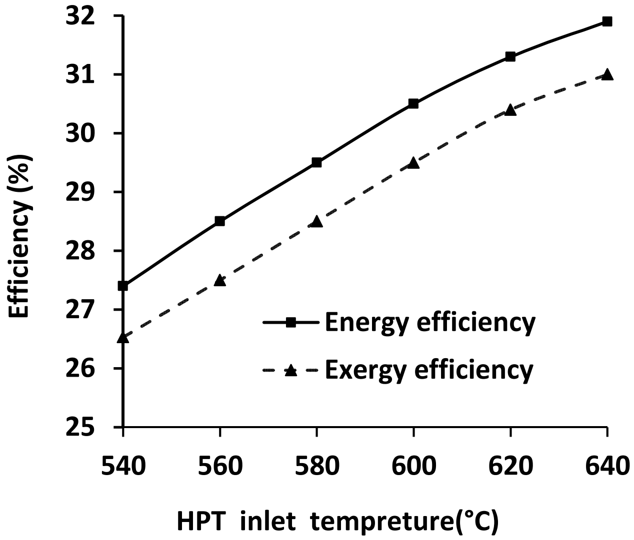

Figure 5 Variations of energy and exergy efficiencies versus HPT inlet temperature

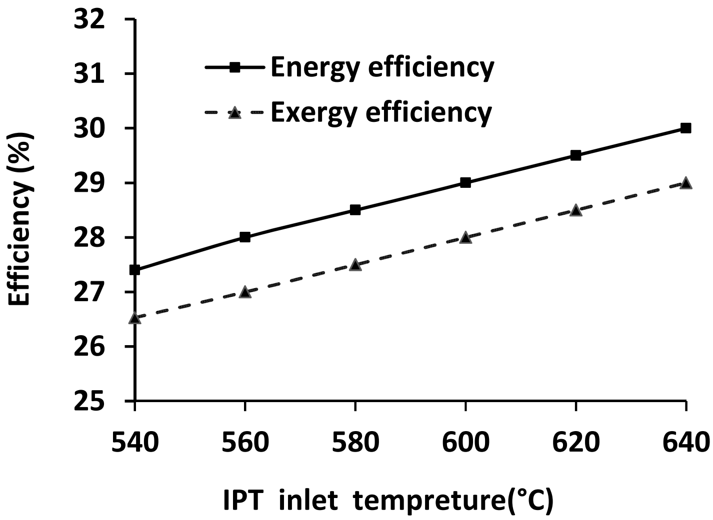

Figure 6 Variations of energy and exergy efficiencies versus IPT inlet temperature

The cycle performance maximizes when the IPT pressure inlet reaches the value of 4.6 MPa. (Figure 7).

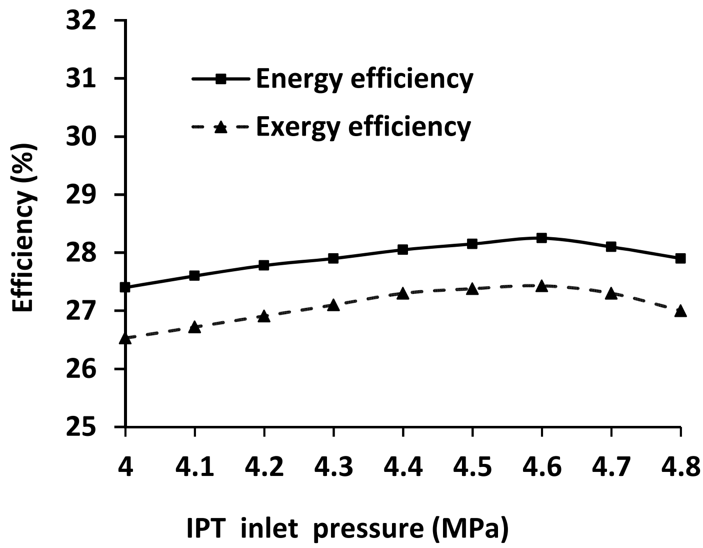

Figure 7 Variations of energy and exergy efficiencies versus IPT inlet pressure

As the area under a curve of T-S diagram represents the net power output, increasing the pressure at IPT inlet at a constant temperature to a certain value leads to a higher net power output, energy and exergy efficiencies. This will cause a reduction in the net power output and the performance cycle.

Changes in net power output based on the input pressure IPT are shown in Figure (8). Since the area under the curve of T-S diagram represents the net output power, increasing the pressure at IPT inlet at a constant temperature to a certain value leads to increasing the net output power, and thereby increasing energy and exergy efficiencies. Higher increase of pressure at IPT at a constant pressure will cause a reduction in the net output power and the cycle performance. Figure (8) shows the changes in net output power versus the pressure at IPT inlet.

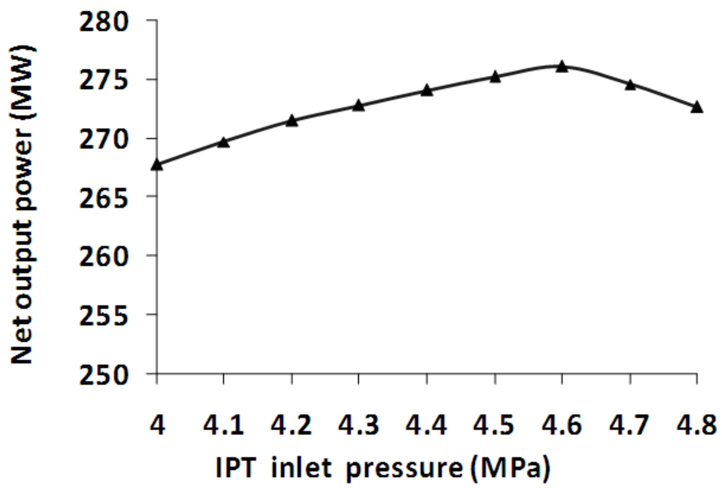

Figure 8 Variations of net power output versus IPT inlet pressure

There is a limitation in increasing the mass flow rate at IPT inlet (Figure 9). The mass flow rate reache*s* the value of about 240 kg/s maximizing the plant performance. Further increase in the mass flow rate results in a decrease in the plant performance.

Increasing the mass flow rate at IPT inlet, considering the constant mass flow rate of the cycle, leads to a decrease in the amount of HPT inlet. This will decrease the portion of the work done by HPT and rise by IPT and LPT. Therefore, the net output work of TUR will increase up to the maximum level of 240 kg/s and then later decrease.

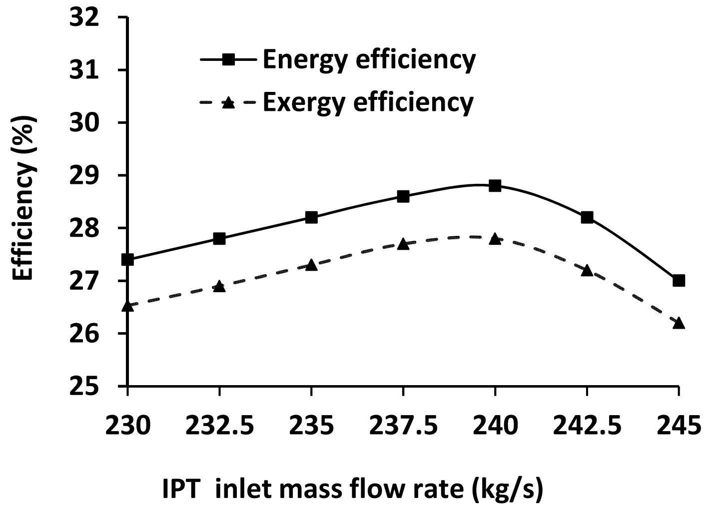

Figure 9 Variations of energy and exergy efficiencies versus IPT inlet mass flow rate

Figure (10) shows the amount of power produced by HPT and LPT versus IPT inlet mass flow rate. The power produced by HPT will decrease with the reduction of mass flow rate and increase with the amount of power generated by the IPT and LPT. The combination of these two graphs shows the net produced power by TUR reaching at the maximum value of 240 kg/s.

Considering the constant mass flow rate of the cycle, increasing the mass flow rate at IPT inlet leads to a decrease in the mass flow rate at HPT inlet. This will decrease the portion of the power done by HPT and increase the power down by IPT and LPT. Therefore, the net output power of TUR will increase up to the maximum level of 240 kg/s and then will decrease. Figures (11) and (12) show the amount of power produced by HPT and the power which is done by HPT and LPT, respectively. The power produced by HPT will decrease with the reduction of mass flow rate and increase with the amount of power generated by the IPT and LPT. The combination of these two graphs shows the net produced power by TUR reaching at the maximum value of 240 kg/s.

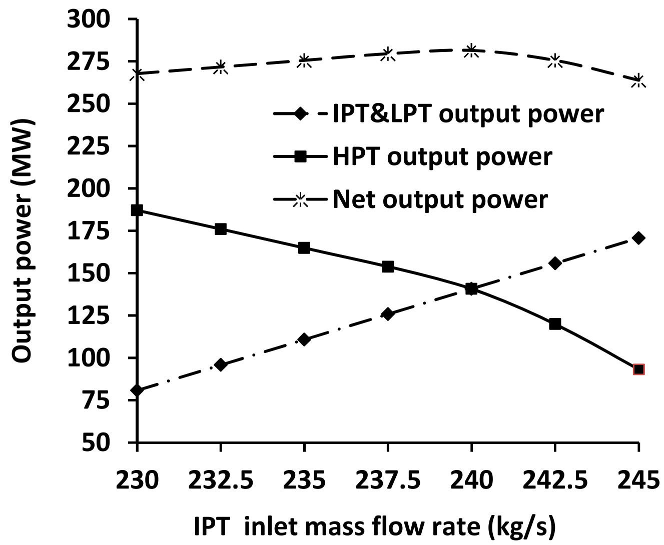

Figure 10 Variation of HPT and LPT net power output versus IPT inlet mass flow rate

The effect of operating conditions is investigated on the exergy destructions of power plant components represented in Figures (11) to (14). Results show that increasing HPT inlet pressure effects only on FWP exergy destruction and exergy destruction of other components remain constant. The same results are observed in Figures (12) to (14).

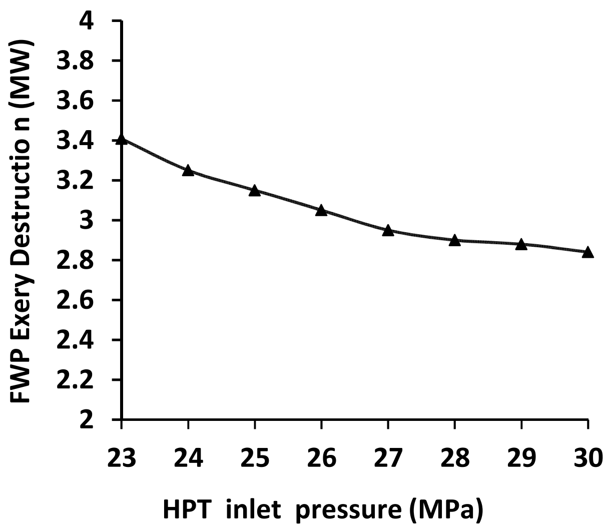

Figure 11 Variations of FWP exergy destruction versus HPT inlet pressure

As shown in Figure (12) when the HPT inlet temperature increases only the exergy destruction of FB decreases and exergy destruction of other components remain constant.

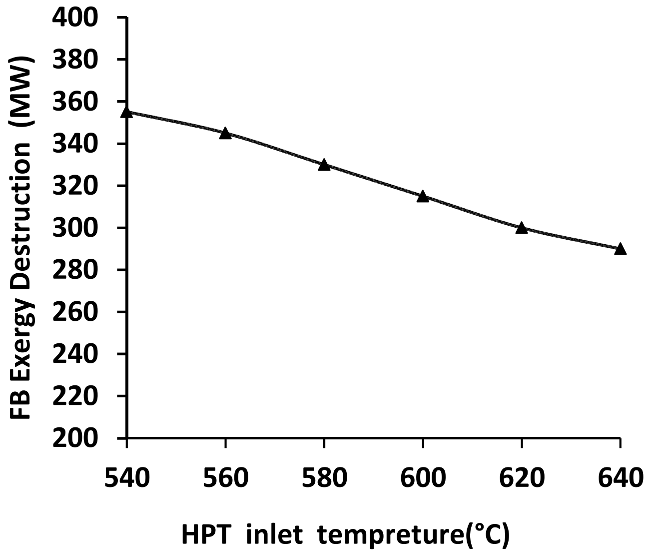

Figure 12 Variations of FB exergy destruction versus HPT inlet temperature

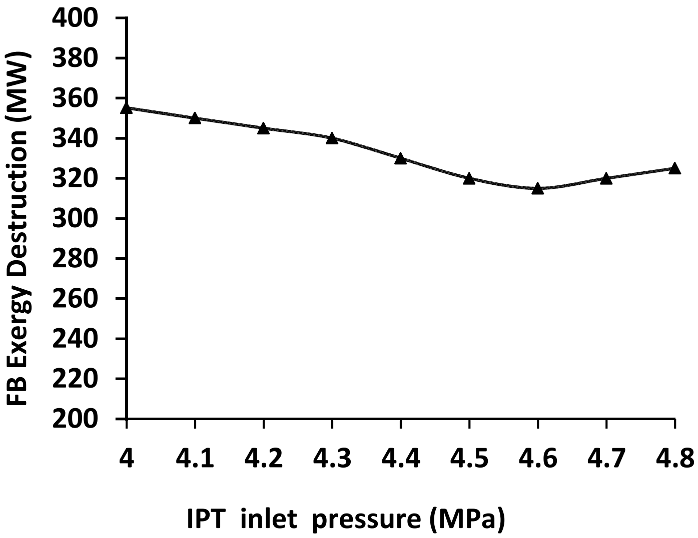

Figure 13 Variations of FB exergy destruction versus IPT inlet pressure

In Figure (13) increasing IPT inlet pressure leads to a decrease in FB exergy destruction to minimum level. The variation of FB exergy destruction is inverse of exergy efficiency in Figure (7). Increasing IPT inlet temperature only leads to a decrease in FB exergy destruction. As shown in Figure (14), as IPT inlet temperature increases, only FB exergy destruction decreases. Also, variation of mass flow rate does not change exergy destruction of plant components.

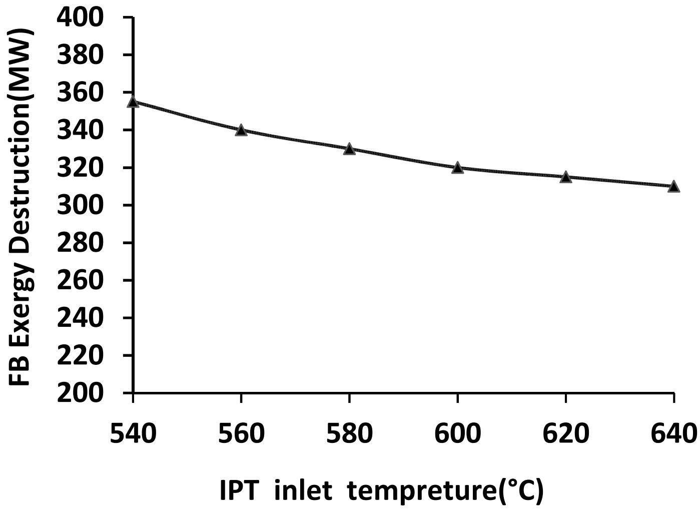

Figure 14 Variations of FB exergy destruction versus IPT inlet temperature

6 Conclusions

This study was performed the energy and exergy analysis as well as the effect of various operating conditions on cycle performance of actual supercritical power plant. The following outcomes were achieved:

- The maximum energy loss is found in the CON where 38.4% of the input energy was lost to the environment. 19% of the energy loss was identified for FB while less than 9% contributes for all other components.
- The total energy efficiency of the cycle is 27.4% based on inlet fuel energy.
- In terms of exergy destruction, the major loss is observed in the FB with the value of 35.2% of the fuel exergy input to the cycle is destroyed. Then, the turbine with the 187.5MW of exergy is vanished representing 18.6% of the fuel exergy input of the cycle.
- The percentage of exergy destruction in CON is 6.4% whereas all other components destroy about 13%.
- The total exergy efficiency of the cycle is 26.5% based on the inlet fuel exergy.
- Cycle performance improves when HPT inlet pressure and temperature and IPT inlet temperature increase. This is Because of the higher energy/exergy content of the greater workoutput of TUR.
- The optimum pressure value of 4.6 MPa is obtained for cycle performance as the IPT inlet pressure increases at inlet temperature and mass flow rate.
- As the IPT inlet mass flow reaches the value of 240 kg/s, the plant performance is maximized.
- Variations of operating conditions effects only on FWP and FB exergy destructions.

References

[1] MAPNA Company, Report, Tehran, Iran, (2008).

[2] Kotas, T., "*The Exergy Method of Thermal Plant Analysis*", London Boston Butterworths, London, (1985).

[3] Bejan, A., Tsatsaronis, G., and Moran, M., "*Thermal Design and Optimization*", Wiley, New York, (1996).

[4] Szargut, J., Morris, D.R., and Steward, F.R., "*Exergy Analysis of Thermal, Chemical, and Metallurgical Processes*", Hemisphere, New York, (1988).

[5] Rosen, M., and Dincer, I., "Exergy as the Confluence of Energy, Environment and Sustainable Development", Exergy International Journal, Vol. 1, No. 1, pp.1–11, (2001).

[6] Dincer, I., and Cengel, Y.A., "Energy, Entropy and Exergy Concepts and their Roles in Thermal Engineering", Entropy, Vol. 3, No. 3, pp.116–149, (2001).

[7] Zubair, S.M., and Habib, M.A., "Second-law-based Thermodynamic Analysis of Regenerative-reheat Rankine-cycle Power Plants", Energy, Vol. 17, pp. 295–301, (1992).

[8] Dincer, I., and Al-Muslim, H., "Thermodynamic Analysis of Reheat Cycle Steam Power Plant", International Journal of Energy Research, Vol. 25, pp. 727–739, (2001).

[9] Verkhivker, G., and Kosoy, B., "On the Exergy Analysis of Power Plants", Energy Conversion and Management, Vol. 42, pp. 2053–2059, (2001).

[10] Rosen, M.A., "Energy and Exergy-based Comparison of Coal-fired and Nuclear Steam Power Plants", International Journal of Exergy, Vol. 3, pp.180–192, (2001).

[11] Suresh, M.V.J.J., Reddy, K.S., and Ajit, K.K., "Energy and Exergy Analysis of Thermal Power Plants Based on Advanced Steam Parameters", International Conference on Advances in Energy Research, India, (2006).

[12] Datta, A., Sengupta S., and Duttagupta S., "Exergy Analysis of a Coal-based 210MW Thermal Power Plant", International Journal of Energy Research, Vol. 31, pp. 14–28, (2007).

[13] Reddy, B.V., and Butcher, C.J., "Second Law Analysis of a Waste Heat Recovery Based Power Generation System", International Journal of Heat and Mass Transfer, Vol. 50, pp. 2355–2363, (2007).

[14] Hasan, H.E., Ali, V.A., Burhanettin, A. D., Suleyman, H.S., Bahri, S., Ismail, T., Cengiz, G., and Selcuk, A., "Comparative Energetic and Exergetic Performance Analyses for Coal-fired Thermal Power Plants in Turkey", International Journal of Thermal Sciences, Vol. 48, pp. 2179–2186, (2009).

[15] Ganapathy, T., Alagumurthi, N., Gakkhar, R.P., and Murugesan, K., "Exergy Analysis of Operating Lignite Fired Thermal Power Plant", Journal of Engineering Science and Technology Review, Vol. 2, pp. 123–130, (2009).

[16] Aljundi Islam, H., "Energy and Exergy Analysis of a Steam Power Plant in Jordan", Applied Thermal Engineering, Vol. 29, pp. 324–328, (2009).

[17] Oktay, Z., "Investigation of Coal-fired Power Plants in Turkey and a Case Study: Can Plant", Applied Thermal Engineering, Vol. 29, pp.550–557, (2009).

[18] Naterer, G.F., Regulagadda, P., and Dincer, I., "Exergy Analysis of a Thermal Power Plant with Measured Boiler and Turbine Losses", Applied Thermal Engineering, Vol. 30, pp. 970–976, (2010).

[19] Kaushik, S.C., Siva Reddy, V., and Tyagi, S.K., "Energy and Exergy Analyses of Thermal Power Plants: A Review", Renewable and Sustainable Energy Reviews, Vol. 15, pp. 1857–1872, (2011).

[20] Hajidavalloo, E., and Vosough, A., "Energy and Exergy Analyses of a Supercritical Power Plant", Int. J. Exergy, Vol. 9, No. 4, pp. 435-452, (2011).

[21] Kanoglu, M., Cengel, Y. A., and Dincer, I., "*Efficiency Evaluation of Energy Systems*", Springer, New York, (2012).

[22] Van Gool, W., "Energy Policy: Fairly Tales and Factualities", in Oares, O.D.D., Martins da Cruz, A., Costa Pereira, G., Soares, I.M.R.T. and Reis, A.J.P.S. (Eds.): Innovation and Technology-Strategies and Policies, Kluwer, Dordrecht, pp. 93–105 (1997).

Nomenclature

$\bar{c}_p$ - Molar specific heat (kJ/kmol. K)
e - Specific energy (kJ/kg)
$\dot{E}$ - Energy rate (kW)
ex - Specific exergy (kJ/ kg)
$\dot{E}x$ - Exergy rate (kW)
h - Specific enthalpy (kJ/kg)
$\bar{h}$ - Molar specific enthalpy (kJ/kmol)
$\bar{h}_f^o$ - Enthalpy of formation (kJ/kmol)
IP - Improvement potential rate (kW)
M- Molar mass (kmol/kg)
$\dot{m}$ - Mass flow rate (kg/s)
P - Pressure (kPa or MPa)
$\bar{R}$ - Universal gas constant (kJ/kmol. K)
s - Specific entropy (kJ/kg K)
$\bar{s}$ - Molar specific entropy (kJ/kmol. K)
T - Temperature (^{o}C or K)
$\dot{W}$ - Power (kW)
x- Mole Fraction(-)

Greek symbols

η - Energy efficiency (%)
ε - Exergy efficiency (%)
φ – Exergy factor

چکیده

تحلیل ترمودینامیکی یک نیروگاه بخار فوق بحرانی با استفاده از مقادیر واقعی به منظور ارزیابی عملکرد و مشخص کردن مکان‌های افت‌های انرژی و تخریب اکسرژی در هر جزء صورت گرفته است. پارامترهای گوناگونی مانند بازده‌های انرژی و اکسرژی، نرخ افت انرژی، نرخ تخریب اکسرژی، نرخ پتانسیل بهبود و بازده‌های مختلف نیروگاه بر اساس قوانین اول و دوم محاسبه و مقایسه شده‌اند. همچنین مطالعه پارامتری برای بررسی اثرات شرایط عملکرد سیستم توربین مانند فشار و دمای ورودی توربین فشار بالا، فشار ورودی توربین فشار متوسط، دمای ورودی توربین فشار بالا، نرخ جریان جرمی ورودی توربین فشار متوسط بر روی بازده‌های نیروگاه و تخریب اکسرژی المانهای مختلف نیروگاه مورد بررسی قرار گرفته است.